BMC Chemistry

RESEARCH

Open Access

Temperature-dependent solubilization and thermodynamic characteristics of ribociclib in varied {PEG 400 + water} combinations

Faiyaz Shakeel[1], Ramadan Al-Shdefat[2], Mohammad Ali[3] and Usama Ahmad[4*]

Abstract

The solubility and thermodynamic characteristics of ribociclib (RCB), a new anticancer medication, have been assessed in a range of {polyethylene glycol 400 (PEG 400) + water} combinations at 293.2–313.2 K and atmospheric pressure. RCB solubility was determined utilizing the saturation shake flask approach, and "van't Hoff, Apelblat, Buchowski-Ksiazczak *λh*, Yalkowsky-Roseman, Jouyban-Acree, and Jouyban-Acree-van't Hoff models" were utilized to validate the measured experimental data. The uncertainties for the computational predictions were less than 3.0% throughout the validation, indicating an outstanding relationship with the experimental RCB solubility data. PEG 400 mass fraction and temperature both improved the solubility of RCB in mole fraction in the compositions of {PEG 400 + water}. It was discovered that the RCB solubility in mole fraction was greatest in pure PEG 400 (1.04×10^{-1}) at 313.2 K and lowest in neat water (1.07×10^{-6} at 293.2 K). All of the {PEG 400 + water} mixes under study showed "endothermic and entropy-driven" RCB dissolution, as indicated by the positive values of the estimated thermodynamic parameters. Compared to RCB-water, RCB-PEG 400 exhibited the strongest molecular interactions. PEG 400 offers a great potential for RCB solubilization in water, according to the evaluation's findings.

Keywords Computational validation, Dissolution, {PEG 400 + water} mixtures, Ribociclib, Solubility, Thermodynamics

Introduction

The crystalline solid known as ribociclib (RCB) (Fig. 1A) is light yellow to yellowish-brown in color [1, 2]. It is a drug that was recently approved to treat metastatic or advanced breast cancer [2]. It is commercialized in the form of a tablet dosage form, containing 200 mg of RCB (as RCB succinate) to treat different stages of breast cancer [2–4]. This drug can also be used as the first endocrine-based treatment in combination with fulvestrant for postmenopausal women with advanced or metastatic breast cancer. The anhydrous succinate salt of RCB is called RCB succinate, and it has a pKa of 5.3 to 8.5 [5, 6]. RCB is a class IV medicine in the biopharmaceutical categorization system (BCS) with low to moderate

*Correspondence:
Usama Ahmad
usamaahmad.10@outlook.com
[1]Department of Pharmaceutics, College of Pharmacy, King Saud University, P.O. Box 2457, Riyadh 11451, Saudi Arabia
[2]Department of Pharmaceutical Sciences, Faculty of Pharmacy, Jadara University, P.O. Box 733, Irbid 21110, Jordan
[3]Department of Pharmacology, Sri Adichunchanagiri College of Pharmacy, Adichunchanagiri University, BG Nagara, Mandya 571448, India
[4]Department of Pharmaceutics, Faculty of Pharmacy, Integral University, Lucknow 226026, India

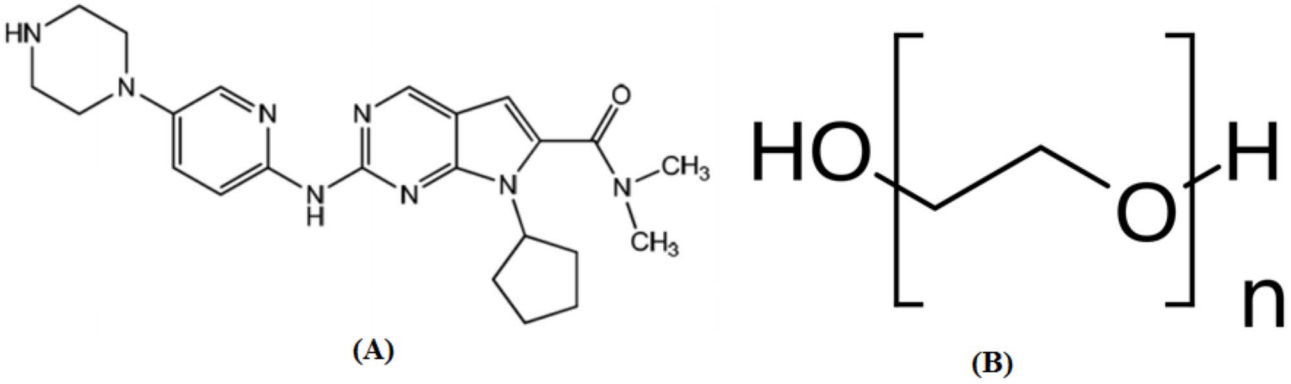

Fig. 1 Molecular structures of (**A**) ribociclib (RCB) (derived from reference [19]) and (**B**) polyethylene glycol 400 (PEG 400) (derived from https://en.wikipedia.org/wiki/PEG_400)

permeability and low solubility in neutral media. Additionally, there is significant inter-subject variability, and achieving appropriate bioavailability can be challenging [1, 6]. Moreover, changes in pH between 2.0 and 7.5 have an inverse relationship with the drug's solubility in an aqueous media [1, 2].

RCB is less sensitive to the pH of gastric fluids and exhibits greater solubility with a pH reduction [1]. The pH of an RCB succinate salt solution at 1.0% w/v in distilled water has been reported to be 5.19. RCB succinate is believed to have low water solubility in neutral medium and a solubility of around 2.4 mg mL^{-1} in acidic conditions, but it is stated to have 0.63 mg mL^{-1} for the free base [1, 6]. It is difficult to develop and commercialize RCB oral formulations due to its poor permeability and solubility. The primary issues with RCB are its low rate of dissolution and restricted bioavailability after oral administration.

For the pharmaceutical industries, drug solubility statistics are crucial [7, 8]. The quality of pharmaceuticals and the success rate of clinical trials can be improved by researchers, particularly those working in the field of medication development and research, by using drug solubility data to make more informed decisions [9]. Moreover, forecasting in vivo pharmacokinetics using solubility data enhances dose prediction [10, 11]. The cosolvency strategy [11] is one method that has been studied in the field of drug discovery to increase the solubility of medications [12–15]. To improve the solubility of RCB, the cosolvent polyethylene glycol 400 (PEG 400) [Fig. 1B] has been used in this study. Enhancing RCB solubility with PEG 400 can help with a variety of RCB problems, such as those related to solubility, absorption, dissolution rate, and bioavailability. A crucial physicochemical element of many industrial processes, such as the creation, manufacturing, and application of dosage forms, is solubility data [16–18]. There is currently insufficient information available regarding the solubility of RCB in mixtures of water and cosolvent. However, its solubility in numerous pure solvents such as water, methanol, ethanol, isopropanol, *n*-butanol, acetone, propylene glycol, PEG 400, Carbitol, ethyl acetate, and dimethyl sulfoxide at 293.2–313.2 K and ambient pressure has been documented [19].

PEG 400 is one of the most widely utilized cosolvents that is frequently used to promote drug solubility because of its perfect miscibility with water [20–22]. Numerous poorly soluble medications, such as emtricitabine, celecoxib, mesalazine, pyridazinone derivatives, pterostilbene, febuxostat, tadalafil, and cyclosporine, have shown promise in becoming more soluble when PEG 400 is added [20–27]. No literature exists that describes the solubilization and thermodynamic behavior of RCB in different combinations of {PEG 400 + water} at certain ambient/atmospheric pressure and temperature. Finding RCB's solubility and thermodynamic characteristics in various {PEG 400 + water} compositions, including pure PEG 400 and water, at temperatures between 293.2 K and 313.2 K under ambient/atmospheric pressure, was the work's main goal. The study's temperature range was selected at random intervals of 5.0 K. In order to ensure that the highest temperature investigated, 313.2 K, did not surpass the boiling temperatures of the solvents or the melting point of the RCB, which is 469.1 K, a temperature range of 293.2 K to 313.2 K was maintained [19]. PEG 400 has a boiling point of 563.2 K, while water has a boiling point of 373.2 K. The greatest temperature evaluated, 313.2 K, was lower than the melting point of RCB and the boiling points of PEG 400 and water. Consequently, the temperature range of the current work stayed within the range mentioned earlier. Data from the study's data gathering phase could be helpful for formulation development, pre-formulation research, and purification of the targeted drug, RCB.

Table 1 Aggregated data for each material utilized

Material	Mol. formula	Mol. weight (g mol^{-1})	CAS	Purification method	Purity (mass fraction)	Analysis method	Source
RCB	$C_{23}H_{30}N_8O$	434.50	1211441-98-3	None	> 0.99	HPLC	Beijing Mesochem
PEG 400	$H(OCH_2CH_2)_nOH$	400.00	25322-68-3	None	> 0.99	HPLC	E-Merck
Water	H_2O	18.07	7732-18-5	None	-	-	Milli-Q

Materials and methods

Materials

RCB standard was obtained from "Beijing Mesochem Technology (Beijing, China)". PEG 400 was obtained from "E-Merck (Darmstadt, Germany)". The water was taken from "Milli-Q unit (Lyon, France)". The aggregated data for every material is shown in Table 1.

Sold state characterization of RCB

For pure RCB (before solubility experiment) and equilibrated RCB (the RCB recovered from bottom phase of equilibrated sample in water), powder X-ray diffraction (PXRD) analyses were carried out to characterize the solid states. Slow evaporation was used to recover the equilibrated RCB from water [19, 24]. For PXRD experiments, the samples were analyzed using a Miniflex 600 Diffractometer (Rigaco, Tokyo, Japan) equipped with Cu–Kα radiation 1.5406 Å. It was operated at 40 kV and 20 mA. With a step size of 0.02°, both pure and equilibrated RCB samples were analyzed in the range of $2\theta = 0–80°$ at a scan rate 3.0000° min^{-1} [24]. The PXRD analyses were used to study the possible transformations of RCB into other physical states, such as polymorphs, solvates, and hydrates, among others.

Table 2 Experimental (x_e) and ideal solubility (x_{idl}) values of RCB in different {PEG 400 + water} mixes (PEG 400 mass fraction $m = 0.0–1.0$) at 293.2–313.2 K and 101.1 kpa

m[a]	x_e[b]				
	T = 293.2 K	T = 298.2 K	T = 303.2 K	T = 308.2 K	T = 313.2 K
0.0	1.14×10^{-5}	1.41×10^{-5}	1.68×10^{-5}	2.11×10^{-5}	2.41×10^{-5}
0.1	2.29×10^{-5}	2.84×10^{-5}	3.41×10^{-5}	4.29×10^{-5}	4.90×10^{-5}
0.2	4.51×10^{-5}	5.59×10^{-5}	6.79×10^{-5}	8.51×10^{-5}	9.89×10^{-5}
0.3	8.91×10^{-5}	1.13×10^{-4}	1.39×10^{-4}	1.74×10^{-4}	2.02×10^{-4}
0.4	1.78×10^{-4}	2.24×10^{-4}	2.73×10^{-4}	3.42×10^{-4}	4.05×10^{-4}
0.5	3.51×10^{-4}	4.40×10^{-4}	5.47×10^{-4}	6.82×10^{-4}	8.17×10^{-4}
0.6	6.90×10^{-4}	8.68×10^{-4}	1.11×10^{-3}	1.41×10^{-3}	1.72×10^{-3}
0.7	1.39×10^{-3}	1.74×10^{-3}	2.20×10^{-3}	2.74×10^{-3}	3.37×10^{-3}
0.8	2.72×10^{-3}	3.43×10^{-3}	4.37×10^{-3}	5.47×10^{-3}	6.73×10^{-3}
0.9	5.37×10^{-3}	6.79×10^{-3}	8.71×10^{-3}	1.12×10^{-2}	1.38×10^{-2}
1.0	1.05×10^{-2}	1.34×10^{-2}	1.73×10^{-2}	2.17×10^{-2}	2.73×10^{-2}
x_{idl}	2.86×10^{-1}	2.99×10^{-1}	3.13×10^{-1}	3.27×10^{-1}	3.41×10^{-1}

[a]The uncertainties u are $u(T) = 0.15$ K, $u(m) = 0.0007$, and $u(p) = 2$ kPa, and [b]the relative uncertainty u_r in solubility is $u_r(x_e) = 0.05$

Determination of RCB solubility in {PEG 400 + water} mixtures and neat solvents

The mass of every {PEG 400 + water} combination was measured using an "Electronic Analytical Balance (Mettler Toledo, Greifensee, Switzerland)" with a sensitivity and accuracy of 0.10 mg. A variety of combinations of {PEG 400 + water} ($m = 0.0–1.0$) were investigated. There were three replications generated for each cosolvent composition [25]. RCB solubilities in numerous {PEG 400 + water} mixtures ($m = 0.1–0.9$), neat PEG 400 ($m = 1.0$), and neat water ($m = 0.0$) were assessed using a shaking flask approach at varied temperatures and constant ambient pressure [28]. Essentially, the excess RCB solids were mixed with triplicates of each cosolvent mix and pure solvent in an unidentified ratio. It required five minutes in total to vortex each combination. To attain equilibrium, the resulting mixes were constantly shaken in an "isothermal water bath (Daihan Scientific Co. Ltd., Seoul, Korea)" for 72 h at 100 rpm [19]. When they had reached equilibrium, the samples were taken out from the shaker and centrifuged for 30 min at 298.2 K at 5000 rpm. After the supernatants were separated and, if necessary, diluted, the concentration of RCB was measured spectrophotometrically at 276 nm [29]. Using common formulae found in the literature, the "experimental mole fraction solubility (x_e)" values for RCB were computed [30–32].

Hansen solubility parameters (HSPs) of RCB and different {PEG 400 + water} mixes

The HSP of a solute is closely connected to how well it dissolves in mixtures of pure or binary solvents. Reports [33] state that when a drug's HSP is comparable to the solvent's, the drug is said to be most soluble in it. This led to the computation of the HSP in this study for RCB, neat PEG 400, neat water, and varied {PEG 400 + water} combinations devoid of RCB. Equation (1) was applied to calculate the total HSP (δ) for RCB and neat solvents (PEG 400 and water) [33–35]:

$$\delta^2 = \delta_d^2 + \delta_p^2 + \delta_h^2 \quad (1)$$

Where, δ = total HSP, δ_d = dispersion HSP, δ_p = polar HSP, and δ_h = hydrogen-bondedn HSP. The HSP data for RCB and neat solvents (PEG 400 and water) were derived from reference [19].

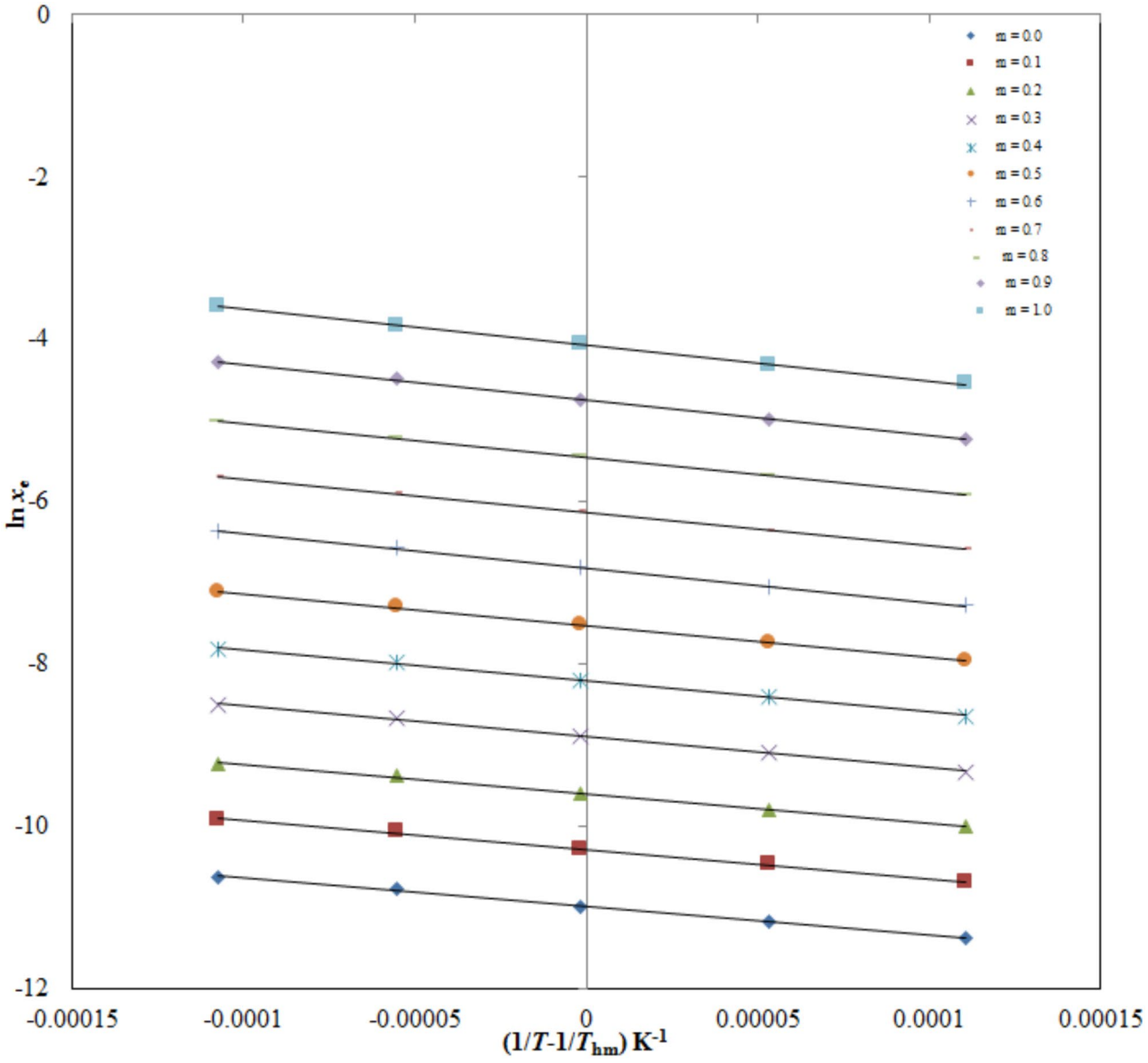

Fig. 2 Van't Hoff graphs to determine the thermodynamic characteristics of RCB in binary {PEG 400 + water} mixtures, created between ln x_e and $1/T\text{-}1/T_{hm}$

Using Eq. (2) [36], the HSP for varied {PEG 400 + water} combinations devoid of RCB (δ_{mix}) was determined:

$$\delta_{mix} = \propto \delta_1 + (1 - \propto)\delta_2 \quad (2)$$

In {PEG 400 + water} compositions, α represents the volume fraction of PEG 400, δ_1 denotes the HSP of PEG 400, and δ_2 denotes the HSP of water.

Molecular interactions based on ideal solubility (x_{idl}) and activity coefficient (γ_i) data

Using Eq. (3), the x_{idl} of RCB at 293.2–313.2 K was calculated [37]:

$$\ln x_{idl} = \frac{-\Delta H_{fus}(T_{fus} - T)}{RT_{fus}T} + \left(\frac{\Delta C_p}{R}\right)\left[\frac{T_{fus} - T}{T} + \ln\left(\frac{T}{T_{fus}}\right)\right] \quad (3)$$

Where ΔC_p is the difference between the molar heat capacity of RCB in its liquid and solid states, ΔH_{fus} is the enthalpy of RCB fusion, R is the universal gas constant, and T is the absolute temperature [38]. The T_{fus}, ΔH_{fus}, and ΔC_p values for RCB are 469.1 K, 10.37 kJ mol^{-1}, and 22.21 J mol^{-1} K^{-1}, respectively, which were taken from the reference [19]. For the validation of T_{fus}, ΔH_{fus}, and ΔC_p values for RCB, the differential scaning calorometry and thermogravimetric analysis spectra for RCB are included in our previous work [19]. Equation (4) was utilized to derive the γ_i values for RCB in all compositions of {PEG 400 + water} and pure solvents [37, 39]:

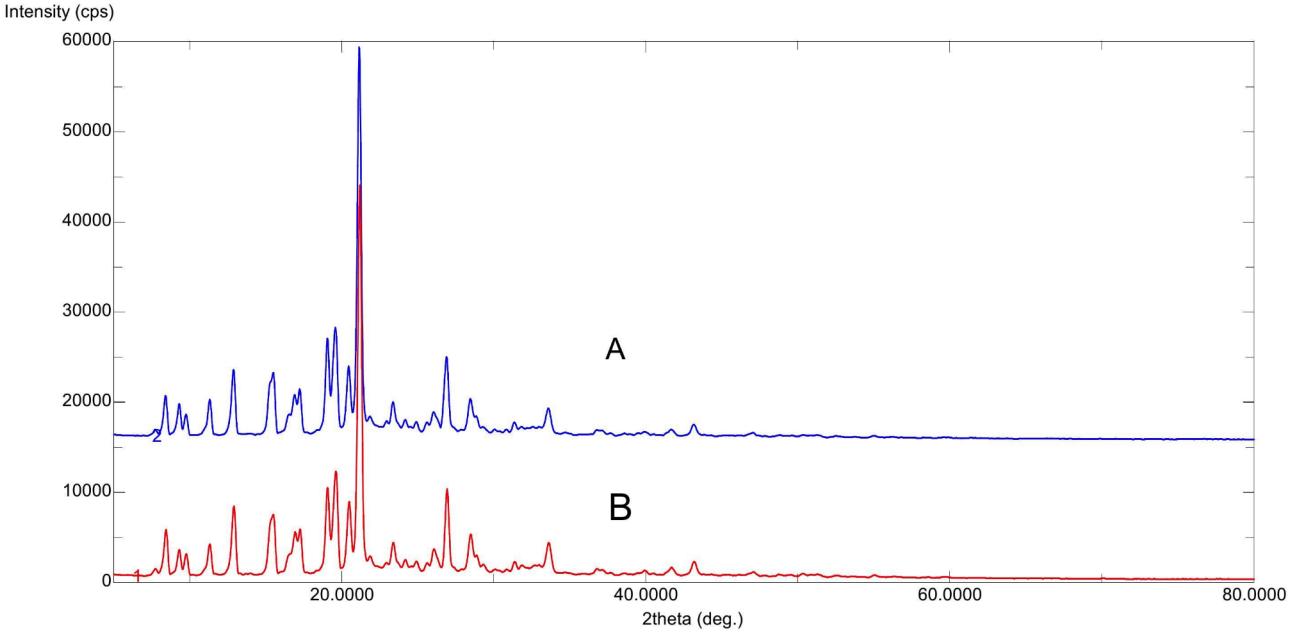

Fig. 3 PXRD spectra of (**A**) pure RCB and (**B**) equilibrated RCB recovered from water

$$\gamma_{\mathrm{i}} = \frac{x_{\mathrm{idl}}}{x_{\mathrm{e}}} \tag{4}$$

RCB γ_i data were utilized to characterize the molecular basis of the interactions between the solvent and solute.

Computational predictions

For forecasts and validations to be useful, solubility data from experiments must be computationally validated [34, 35]. To evaluate the RCB experimental solubility data, six different computational techniques were employed: "van't Hoff, Apelblat, Buchowski-Ksiazczak λh, Yalkowsky-Roseman, Jouyban-Acree, and Jouyban-Acree-van't Hoff models" [25, 40–45]. The descriptions of every computation are provided below:

Van't Hoff model

The "van't Hoff model solubility ($x^{\mathrm{van't}}$)" of RCB in various {PEG 400 + water} compositions, including pure solvents, was estimated by Eq. (5) [25]:

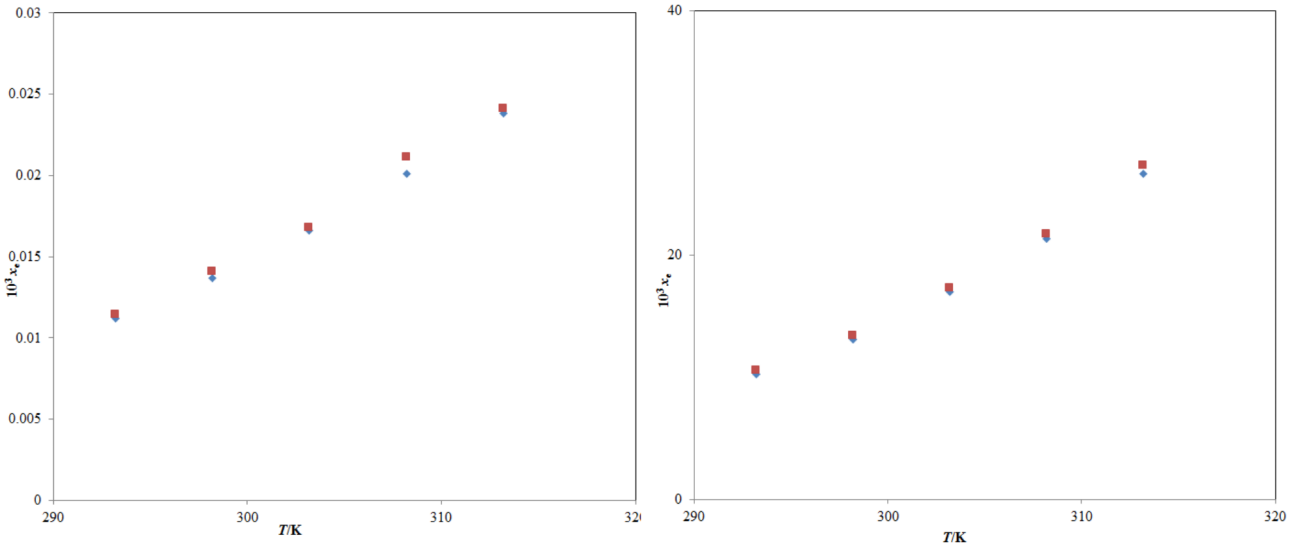

Fig. 4 RCB experimental mole fraction solubility (x_e) data in (**A**) neat water and (**B**) neat PEG 400 are graphically compared to those published in the literature at 293.2–313.2 K. The symbol ■ represents the x_e values of RCB in (**A**) neat water and (**B**) neat PEG 400, and the symbol ◆ indicates the reported solubilities of RCB in (**A**) neat water and (**B**) neat PEG 400 derived from reference [19]

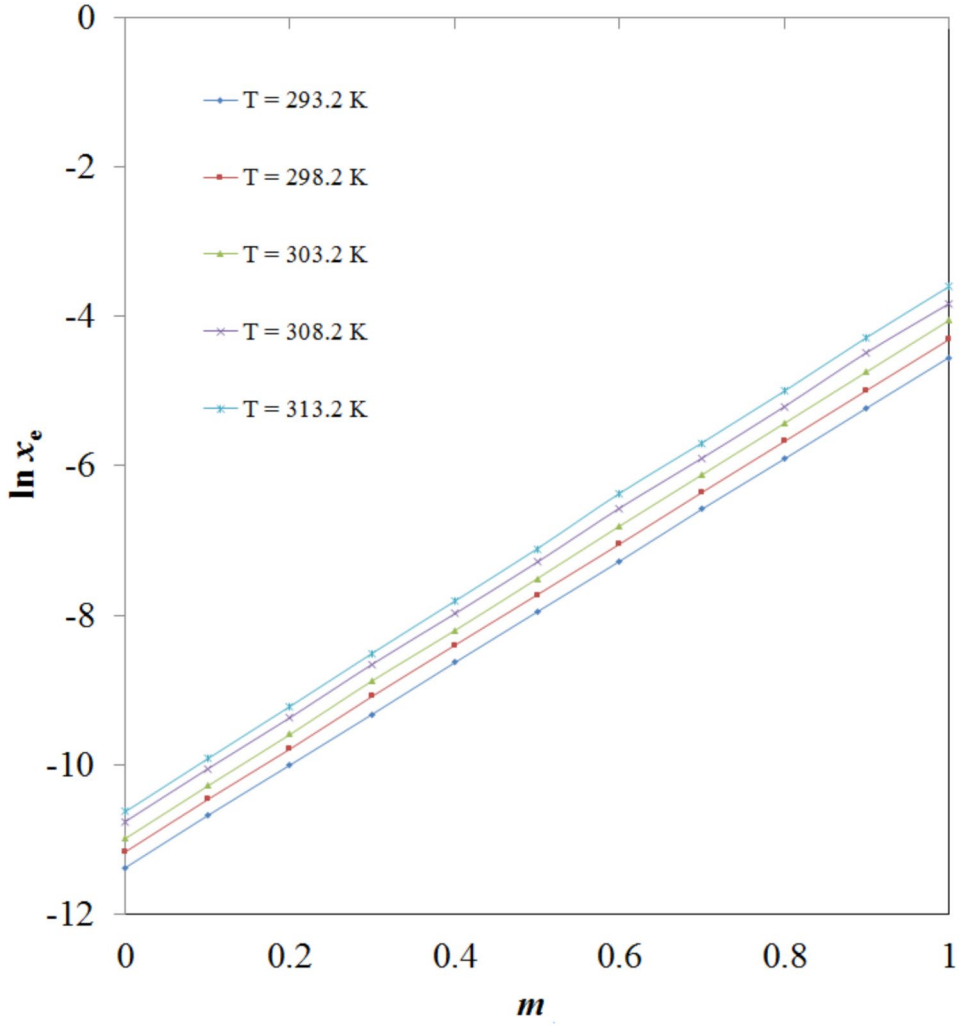

Fig. 5 The effect of PEG 400 mass fraction (*m*) on RCB ln x_e values at five different temperatures ranged from 293.2 K to 313.2 K

$$\ln x^{\mathrm{van't}} = a + \frac{b}{T} \tag{5}$$

Table 3 RCB activity coefficients (γ_i) data at 293.2–313.2 K in varied {PEG 400 + water} mixes (*m* = 0.0–1.0)

m	γ_i				
	T = 293.2 K	T = 298.2 K	T = 303.2 K	T = 308.2 K	T = 313.2 K
0.0	25,138	21,267	18,615	15,478	14,156
0.1	12,506	10,549	9200.9	7636.6	6964.8
0.2	6355.6	5367.1	4614.8	3847.3	3453.8
0.3	3215.7	2646.1	2247.2	1877.7	1694.4
0.4	1612.4	1338.2	1147.9	956.88	843.34
0.5	817.52	681.07	572.64	479.93	418.29
0.6	415.47	345.30	283.41	232.79	199.10
0.7	206.75	172.76	142.67	119.28	101.50
0.8	105.55	87.376	71.667	59.853	50.720
0.9	53.374	44.100	35.955	28.992	24.717
1.0	27.126	22.304	18.041	15.078	12.507

Where *a* and *b* represent the model parameters from Eq. (5) that were obtained using the least squares method [30]. The x_e and $x^{\mathrm{van't}}$ data for the RCB were correlated using the "root mean square deviation (*RMSD*)". The *RMSD* was calculated using a formula that was obtained from the literature [46].

Apelblat model

The "Apelblat model solubility (x^{Apl})" of RCB in cosolvent mixtures and neat solvents was calculated using Eq. (6) [40, 41]:

$$\ln x^{\mathrm{Apl}} = A + \frac{B}{T} + C\ln(T) \tag{6}$$

Where *A*, *B*, and *C* represent the model parameters from Eq. (6) that were computed by the "nonlinear multiple regression analysis" of the RCB x_e values listed in Table 2

Table 4 Results for the "van't Hoff model" with model parameters (*a* and *b*), R^2, and *RMSD* for RCB in various {PEG 400 + water} mixes (*m* = 0.0–1.0)

m	a	b	R^2	Overall RMSD (%)
0.0	0.56420	−3500.7	0.9960	
0.1	1.4354	−3551.4	0.9962	
0.2	2.4772	−3659.2	0.9979	
0.3	3.6274	−3793.4	0.9962	
0.4	4.3474	−3804.5	0.9988	
0.5	5.3891	−3911.6	0.9994	1.29
0.6	7.1531	−4232.6	0.9994	
0.7	7.3994	−4100.0	0.9998	
0.8	8.3941	−4193.8	0.9998	
0.9	9.7891	−4404.4	0.9991	
1.0	10.339	−4369.0	0.9998	

[30]. The values of x_e and x^{Apl} for the RCB were linked using the *RMSD*.

Buchowski-Ksiazczak λh model

The "Buchowski-Ksiazczak λh solubility ($x^{\lambda h}$)" of RCB in various {PEG 400 + water} compositions, including pure solvents, was estimated using Eq. (7) [42, 43]:

$$\ln\left[1+\frac{\lambda\left(1-x^{\lambda\,\mathrm{h}}\right)}{x^{\lambda\,\mathrm{h}}}\right]\;=\;\lambda\,h\,[\frac{1}{T}-\frac{1}{T_{\mathrm{fus}}} \tag{7}$$

The model parameters, represented by λ and h, originate from Eq. (7).

Yalkowsky-Roseman model

The solubility data of pharmaceuticals in cosolvent mixes at diverse solvent combinations cannot be obtained since Eqs. (5–7) describe solubility data at different temperatures in a particular solvent combination [45, 46]. It is necessary to employ cosolvency techniques such as "Yalkowsky-Roseman, Jouyban-Acree, and Jouyban-Acree-van't Hoff models". Equation (8) was utilized to calculate the "logarithmic solubility of Yalkowsky-Roseman model (log x^{Yal})" for RCB in various cosolvent compositions [44]:

$$\log x^{\mathrm{Yal}}=w_1\log x_1+w_2\log x_2 \tag{8}$$

Where, x_1 and x_2 represent the solubility of RCB in PEG 400 and water, respectively, and w_1 and w_2 represent the mass fractions of PEG 400 and water, respectively. Equation (8) connects drug solubility data in different solvent combinations at a given temperature.

Jouyban-Acree model

The "Jouyban-Acree model" solubility of RCB ($x_{m,T}$) at various cosolvent combinations and temperatures was estimated using Eq. (9) [44]:

$$\ln x_{m,T}=w_1\ln x_{1,T}+w_2\ln x_{2,T}+(\frac{w_1.w_2}{T})\sum_{i=0}^{2}J_i(w_1-w_2)^i \tag{9}$$

Where, J_i is the model parameter from Eq. (9), and $x_{1,T}$ and $x_{2,T}$ are RCB solubility in PEG 400 and water, respectively. Equation (10) can be used to characterize the trained form of Eq. (9) for the current data set by adding the J_i value:

$$\ln x_{\mathrm{m},\mathrm{T}}\;=w_1\ln x_1+\;w_2\ln x_2+\;\frac{62335w_1\,w_2}{T} \tag{10}$$

Jouyban-Acree-van't Hoff model

When determining the RCB solubility in different cosolvent mixes at a particular temperature, the RCB solubility values in pure PEG 400 and water must be utilized as input data. To overcome this limitation, the "Jouyban-Acree-van't Hoff model" (Eq. 11) can be formed using Eqs. (5) and (9) [45]:

$$\begin{array}{l}\ln x_{\mathrm{m},\mathrm{T}}=w_1\left(A_1+\frac{B_1}{T}\right)\\+w_2\;\left(A_2+\;\frac{B_2}{T}\right)+\left[\frac{w_1w_2}{T}\;\sum\;{}_{i=0}^{2}J_{\mathrm{i}}\left(w_1-w_2\right)\right]\end{array} \tag{11}$$

Where the model parameters in Eq. (11) are A_1, B_1, A_2, B_2, and J_i. The trained version of Eq. (11) for the present data set can be stated by Eq. (12):

$$\begin{array}{l}\ln x_{\mathrm{m},\mathrm{T}}=w_1\left(10.349-\;\frac{4369.0}{T}\right)\\+w_2\;\left(0.56420-\;\frac{3500.7}{T}\right)+\;\frac{60876w_1w_2}{T}\end{array} \tag{12}$$

Thermodynamic parameters

All of the apparent thermodynamic parameters of the RCB were calculated using the "mean harmonic temperature (T_{hm})" [37]. The given equation was used to derive the T_{hm} [37, 45]. The T_{hm} for RCB, as established by us, is 306 K. A variety of thermodynamic parameters were obtained by means of an apparent thermodynamic investigation. The "van't Hoff and Gibbs equations" were used to compute these parameters. Equation (13) was used to calculate the "apparent standard enthalpy ($\Delta_{sol}H^0$)" values for RCB at T_{hm} = 306 K in cosolvent compositions and pure solvents [37, 47]:

$$\left(\frac{\partial\ln x_{\mathrm{e}}}{\partial\left(1/T-1/T_{\mathrm{hm}}\right)}\right)_P\;=\;-\frac{\Delta_{\mathrm{sol}}H^0}{R} \tag{13}$$

The created "van't Hoff" graphs between ln x_e of RCB and $1/T-1/T_{hm}$ yielded the "$\Delta_{sol}H^0$" for RCB. Figure 2 shows the van't Hoff graphs for RCB in pure solvent and cosolvent combinations.

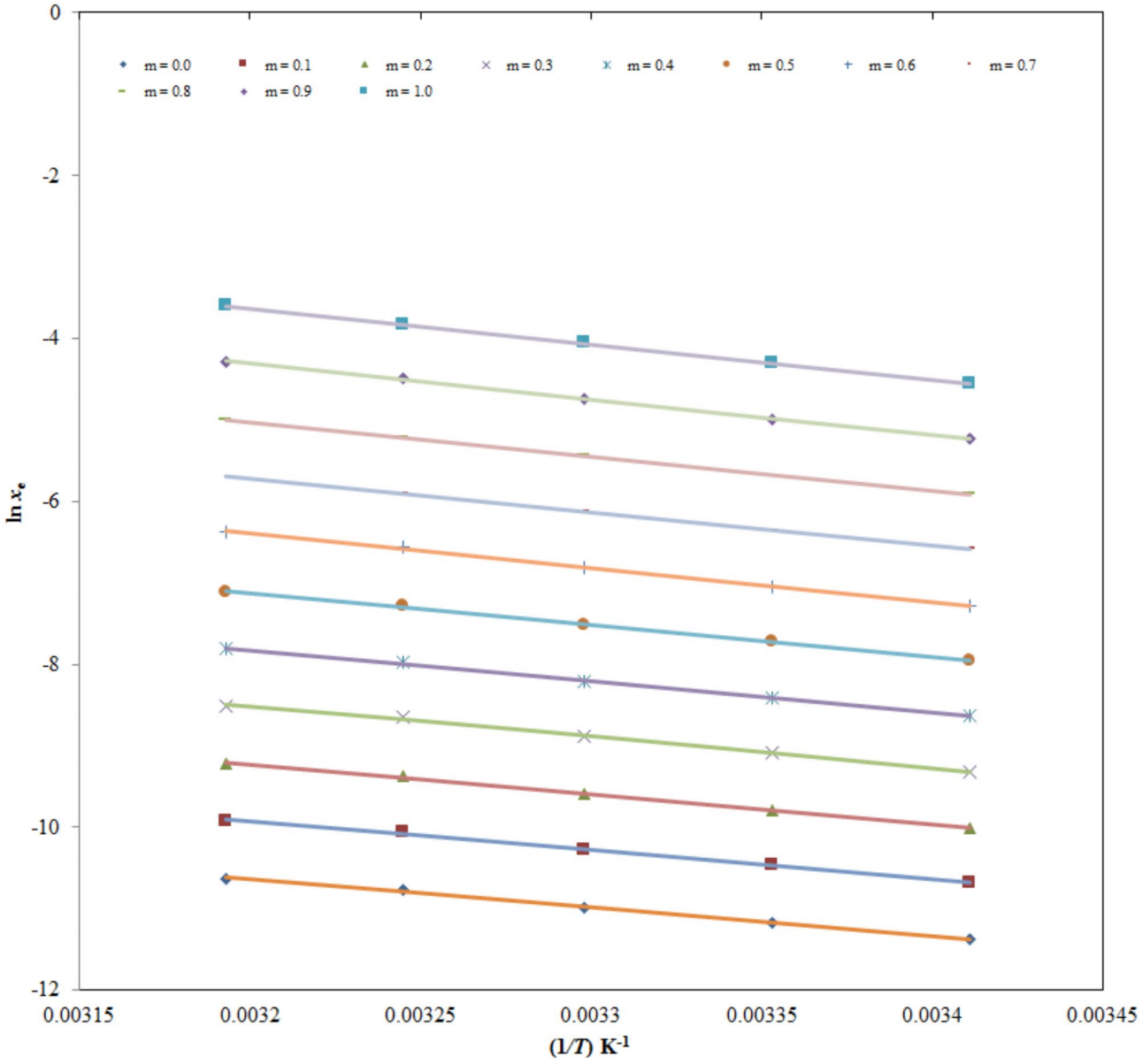

Fig. 6 A graph illustrating the relationship between RCB x_e values and the "Apelblat model" for a variety of {PEG 400 + water} compositions (m = 0.0–1.0) plotted against 1/T. Solid lines indicate the RCB x_e values, while symbols represent the RCB solubility values from the "Apelblat model."

Furthermore, the "apparent standard Gibbs energy ($\Delta_{sol}G^0$)" for RCB in varied cosolvent compositions and pure solvents at T_{hm} = 306 K was estimated by Krug et al. approach using Eq. (14) [47].

$$\Delta_{sol}G^0 = -RT_{hm} \times \text{intercept} \quad (14)$$

In which the RCB intercept values in varied cosolvent compositions and neat solvents were determined by the "van't Hoff plots" shown in Fig. 2.

Equation (15) was used to get the "apparent standard entropies ($\Delta_{sol}S^0$)" for RCB in varied cosolvent compositions and pure solvents [37, 47, 48]:

$$\Delta_{sol}S^0 = \frac{\Delta_{sol}H^0 - \Delta_{sol}G^0}{T_{hm}} \quad (15)$$

Results and discussion

Solid state characterization of RCB

In order to evaluate the polymorph/solvates/hydrates of the RCB, PXRD analyses were used to characterize the solid states of RCB in pure and equilibrated samples. Figure 3 depicts the PXRD spectra of pure and equilibrated RCB (recovered from water). The PXRD spectra of pure RCB indicated multiple crystalline peaks of RCB at varied 2θ angles, indicating that pure RCB is crystalline (Fig. 3A). The PXRD spectra of equilibrated RCB

Table 5 Results of the "apelblat model" with model parameters (*A*, *B*, and *C*), R^2, and *RMSD* for RCB in varied {PEG 400 + water} mixes ($m = 0.0–1.0$)

m	A	B	C	R^2	Overall RMSD (%)
0.0	96.527	−7835.1	−14.290	0.9961	
0.1	101.30	−8061.9	−14.871	0.9963	
0.2	63.105	−6398.4	−9.0282	0.9978	
0.3	271.45	−15,887	−39.886	0.9978	
0.4	90.516	−7697.1	−12.832	0.9989	
0.5	68.847	−6778.8	−9.4496	0.9994	0.99
0.6	−39.451	−2130.5	6.9421	0.9993	
0.7	−37.164	−2090.1	6.6382	0.9997	
0.8	8.1430	−4184.7	0.03873	0.9997	
0.9	−75.752	−544.43	12.741	0.9989	
1.0	−21.506	−2933.2	4.7456	0.9997	

also showed identical peaks of RCB at different 2θ angles (Fig. 3B), indicating that equilibrated RCB is also crystalline. Overall, the PXRD spectra indicated that following equilibrium, RCB was not transformed into polymorphs/solvates/hydrates.

Comparing literature and RCB measured solubility data

The measured RCB solubility values at 293.2–313.2 K and 101.1 kPa are summarized in Table 2 for both pure solvents and binary {PEG 400 + water} compositions.

There is no information available on the solubility of RCB in binary {PEG 400 + water} combinations at varying temperatures. However, solubility statistics have been reported for RCB in mole fraction in water and pure PEG 400 at 293.2–313.2 K [19]. The solubility values of RCB in pure PEG 400 and water at 293.2–313.2 K are compared to the reported values shown in Fig. 4. The solubility values of RCB in pure water and PEG 400, as acquired by experimentation, show a strong consistency with the reported data presented in Fig. 4 [19]. These findings showed that the solubility statistics from RCB that were measured experimentally corresponded well with previously published information [19]. It was commonly estimated that the RCB solubilities were greatest in pure PEG 400 and least in water. The reason RCB dissolves more completely in pure PEG 400 could be due to PEG 400's weaker polarity than water [24–26]. The reason for RCB's higher solubility in PEG 400 could potentially be attributed to intermolecular interactions between the C = O and -NH groups of RCB (Fig. 1A) and the many -OH groups of PEG 400 (Fig. 1B). In binary mixes of PEG 400 and water, the solubility of RCB was increased with temperature and PEG 400 mass fraction. The solubility of RCB in logarithmic mole fractions at five different temperatures was also examined in connection to the PEG 400 mass fraction. The results are summarized in Fig. 5. In all cosolvent solutions and at all investigated temperatures, RCB solubility rose linearly with the PEG 400 mass fraction.

The results of effect of temperature and PEG 400 mass fraction on RCB solubility were in accordance with those reported for several hydrophobic compounds such as, emtricitabine, celecoxib, mesalazine, pyridazinone derivatives, pterostilbene, febuxostat, tadalafil, and cyclosporine [20–27]. These results imply that RCB is soluble in PEG 400 and slightly soluble in water. Consequently, PEG 400 was determined to be the optimal solvent for RCB and water to be the antisolvent. Compared to pure water, the solubility of RCB in mole fractions increased significantly to neat PEG 400. As a result, PEG 400 can be used as a cosolvent to dissolve RCB in an aqueous media such as water. All things considered, PEG 400 can be used as a cosolvent in pre-formulation studies and dosage form development for RCB, particularly when it comes to liquid dosage forms.

Prediction of HSPs

HSPs provide a quantitative assessment of the degree of interaction between the solute and the solvent, making them an effective tool for determining miscibility or solubility [33]. Solutes and solvents are likely to dissolve in one another, according to similar HSPs [34]. The solvent and the solute share the same polarity, as further demonstrated by the identical HSPs. Thus, the HSPs of RCB, neat PEG 400, and water were calculated in this study. The HSPs estimation has multiple applications across multiple research disciplines [33, 34]. The primary goal of the current experiment was to collect data on the solvent and solute's solubility. The δ value for RCB was derived to be 25.10 $MPa^{1/2}$ by using reference [19], which suggests low polarity. HSP values of 18.90 $MPa^{1/2}$ and 47.80 $MPa^{1/2}$, respectively, were derived for neat PEG 400 (δ_1) and water (δ_2). The HSP range for binary {PEG 400 + water} compositions without RCB (δ_{mix}) was determined to be 21.79–44.91 $MPa^{1/2}$. It was found that the δ_{mix} values in the {PEG 400 + water} compositions declined as the mass fraction of PEG 400 rose. Consequently, $m = 0.1$ and $m = 0.9$ yielded the highest and lowest δ_{mix} values, respectively. However, it was discovered that the RCB solubility values were enhanced by lowering the δ_{mix} values. The HSPs of RCB ($\delta = 25.10$ $MPa^{1/2}$) and pure PEG 400 ($\delta_1 = 18.90$ $MPa^{1/2}$) were in close proximity to one another. The investigations also revealed that RCB dissolves more easily in pure PEG 400. Consequently, these outcomes agreed well with the RCB solubility data obtained from experiments using mixtures of {PEG 400 + water}.

Molecular interactions based on x_{idl} and γ_i

The RCB x_{idl} values are listed in Table 2. At 293.2–313.2 K, the obtained values for RCB's x_{idl} varied from

2.86×10^{-1} to 3.41×10^{-1}. The x_e values in neat water were significantly lower than the x_{idl} levels of RCB. The x_e values of RCB in pure PEG 400 were nearly equal to the x_{idl} values of RCB at all tested temperatures. Pure PEG 400 dissolves RCB more easily, hence this cosolvent is suitable for RCB solubilization. The γ_i values for RCB at 293.2–313.2 K are shown in Table 3 for a range of {PEG 400 + water} mixes, and pure solvents. The RCB's γ_i value in pure water reached its maximum value at every temperature that was tested. At every temperature examined, the pure PEG 400 had the lowest RCB γ_i. The γ_i results for RCB in neat PEG 400 were significantly lower than those for pure water. The highest γ_i for RCB in pure water could potentially be explained by its lowest water solubility. These findings suggest that the RCB-PEG 400 combination exhibits more molecular solute-solvent interactions than the RCB-water combination.

Computational predictions

Six different computational models, such as, the "van't Hoff, Apelblat, Buchowski-Ksiazczak λh, Yalkowsky-Roseman, Jouyban-Acree, and Jouyban-Acree-van't Hoff models" [25, 40–45], were used to validate the RCB solubility data.

Van't Hoff model

The model fitting results utilizing the "van't Hoff model" are shown in Table 4. This model's overall *RMSD* was calculated to be 1.29%. The findings demonstrated that all cosolvent compositions and pure solvents had RCB coefficients of determination (R^2) that ranged from 0.9960 to 0.9998. In a variety of cosolvent compositions, including neat solvents, there were strong correlations seen between the predictions of the "van't Hoff model" and the experimental solubility data obtained for the RCB. The correlation results of this model were in accordance with those reported for emtricitabine, pyridazinone derivatives, pterostilbene, and febuxostat [20, 23–25].

Table 6 Results of "Buchowski-Ksiazaczak *λh* model" with model parameters (*λ* and *h*), R^2, and *RMSD* for RCB in varied {PEG 400 + water} mixes (*m* = 0.0–1.0)

m	λ	h	R^2	Overall RMSD (%)
0.0	5.89810	593.564	0.9960	
0.1	5.13500	691.645	0.9962	
0.2	4.32340	846.370	0.9979	
0.3	3.45910	1096.64	0.9962	
0.4	2.76290	1377.03	0.9988	
0.5	1.94950	2006.51	0.9994	2.78
0.6	0.869500	4867.85	0.9994	
0.7	0.340700	12033.7	0.9998	
0.8	0.454100	9235.41	0.9998	
0.9	0.600000	7340.67	0.9991	
1.0	0.035300	123,767	0.9998	

Apelblat model

The experimental and Apelblat solubility data for RCB in a range of cosolvent compositions, including neat solvents, are graphically compared in Fig. 6. The findings shown in Fig. 6 showed a robust connection between the experimentally acquired solubility data of RCB and the "Apelblat model." These correlation results were in accordance with those reported for emtricitabine, pyridazinone derivatives, pterostilbene, and febuxostat [20, 23–25]. Table 5 presents the correlation values obtained with the "Apelblat model". This model's calculated overall *RMSD* was 0.99%. The results demonstrated that all cosolvent compositions and pure solvents had RCB R^2 values between 0.9961 and 0.9997. The RCB's experimental solubility data showed a good agreement with the "Apelblat model" predictions across a range of cosolvent compositions and neat solvents.

Buchowski-Ksiazaczak λh model

Table 6 displays the correlation results using the "Buchowski-Ksiazaczak *λh*" model. This model's calculated overall *RMSD* was 2.78%. The results showed that the range of RCB R^2 was 0.9960 to 0.9998 for all cosolvent compositions and pure solvents. In a range of cosolvent compositions and pure solvents, the experimental solubility data from the RCB demonstrated a strong connection with the predictions of the "Buchowski-Ksiazaczak *λh*" model.

Yalkowsky-Roseman model

Table 7 displays the correlation results using the "Yalkowsky-Roseman model". The overall *RMSD* of this model was estimated to be 1.52%. In every cosolvent composition, a significant correlation was seen between the experimental solubility data obtained from the RCB and the predictions of the "Yalkowsky-Roseman model". The correlation results of "Yalkowsky-Roseman model" were in accordance with those reported for emtricitabine, pyridazinone derivatives, pterostilbene, and febuxostat [20, 23–25].

Jouyban-Acree and Jouyban-Acree-van't Hoff models

Furthermore, "Jouyban-Acree and Jouyban-Acree-van't Hoff models" were connected to the solubility data of RCB in a variety of cosolvent solutions at a range of compositions and temperatures [45]. The association between the "Jouyban-Acree and Jouyban-Acree-van't Hoff models" is seen in Table 8. The overall *RMSDs* for the "Jouyban-Acree and Jouyban-Acree-van't Hoff models," which are 0.87% and 0.93%, respectively, show an outstanding association, according to the model's expectations. The correlation results of "Jouyban-Acree and Jouyban-Acree-van't Hoff models" were in accordance with those reported for emtricitabine, pyridazinone derivatives,

Table 7 Results of "Yalkowsky-Roseman model" for RCB in varied {PEG 400 + water} mixtures ($m = 0.1–0.9$) at 293.2 K to 313.2 K

m	Log x^{Yal}					Overall RMSD (%)
	T = 293.2 K	T = 298.2 K	T = 303.2 K	T = 308.2 K	T = 313.2 K	
0.1	-4.64	-4.55	-4.47	-4.37	-4.31	
0.2	-4.34	-4.25	-4.17	-4.07	-4.04	
0.3	-4.05	-3.95	-3.86	-3.77	-3.70	
0.4	-3.75	-3.65	-3.56	-3.47	-3.39	
0.5	-3.45	-3.36	-3.26	-3.16	-3.09	1.52
0.6	-3.16	-3.06	-2.96	-2.86	-2.78	
0.7	-2.86	-2.76	-2.66	-2.56	-2.47	
0.8	-2.56	-2.46	-2.36	-2.26	-2.17	
0.9	-2.27	-2.16	-2.06	-1.96	-1.86	

Table 8 Results of "Jouyban-Acree" and "Jouyban-Acree-van't Hoff" models for RCB in different {PEG 400 + water} compositions

System	Jouyban-Acree	Jouyban-Acree-van't Hoff
		A_1 10.349
		B_1 −4369.0
{PEG 400 + water}	J_i 62,335	A_2 0.56420
RMSD (%)	0.87	B_2 −3500.7
		J_i 60,876
		0.93

Table 9 Apparent thermodynamic parameters ($\Delta_{sol}H^0$, $\Delta_{sol}G^0$, and $\Delta_{sol}S^0$) along with R^2 for RCB in varied {PEG 400 + water} compositions ($m = 0.0–1.0$)[c]

m	$\Delta_{sol}H^0$/kJ mol^{-1}	$\Delta_{sol}G^0$/kJ mol^{-1}	$\Delta_{sol}S^0$/J mol^{-1} K^{-1}	R^2
0.0	29.09	27.68	4.67	0.9960
0.1	29.52	25.90	11.91	0.9962
0.2	30.41	24.18	20.57	0.9979
0.3	31.53	22.39	30.13	0.9962
0.4	31.62	20.67	36.12	0.9988
0.5	32.51	18.94	44.78	0.9994
0.6	35.18	17.16	59.44	0.9994
0.7	34.08	15.44	61.49	0.9998
0.8	34.86	13.71	69.76	0.9998
0.9	36.61	11.95	81.36	0.9990
1.0	36.31	10.25	86.01	0.9998

[c]The relative uncertainties are $u(\Delta_{sol}H^0) = 0.008$, $u(\Delta_{sol}G^0) = 0.030$, and $u(\Delta_{sol}S^0) = 0.060$

pterostilbene, and febuxostat [20, 23–25]. Low *RMSD* values across all models suggested a strong overall correlation. Comparing the error levels of each model to one another, however, was not practicable. The error levels of all the models under consideration fell between a defined range of the experimental uncertainties. This result showed that every model tested could reliably reproduce the experiment's solubility data with the least amount of error.

Thermodynamic evaluation of RCB dissolution

The $\Delta_{sol}H°$ values for RCB in various cosolvent compositions and pure solvents were computed using the van't Hoff method. Table 9 shows that for the linear van't Hoff curves of RCB in different cosolvent compositions, PEG 400, and water (Fig. 2), $R^2 > 0.99$ was expected. The outcomes for every thermodynamic parameter are also shown in Table 9. The values of RCB $\Delta_{sol}H°$ in neat solvents and cosolvent mixtures ranged from 29.09 to 36.61 kJ mol^{-1}. The values of RCB $\Delta_{sol}G°$ in neat solvents and cosolvent mixtures ranged from 10.25 to 27.68 kJ mol^{-1}. The RCB exhibited "endothermic dissolution" in a variety of cosolvent compositions, including neat solvents, according to the $\Delta_{sol}H°$ and $\Delta_{sol}G°$ data [24, 25].

The values of RCB $\Delta_{sol}S°$ in neat solvents and different cosolvent compositions ranged from 4.67 to 86.01 J mol^{-1} K^{-1}. The RCB's $\Delta_{sol}S°$ measurements showed that it dissolved "entropy-driven" in a variety of cosolvent compositions, including neat solvents [24]. It has since been found that RCB dissolved in a variety of cosolvent compositions, including neat solvents, in a "endothermic and entropy-driven" manner [24, 25].

Conclusions

RCB's solubility statistics in any of the {PEG 400 + water} combinations are unknown as of yet. RCB's solubility was examined in this work at fixed pressures and different temperatures in a variety of PEG 400 aqueous solutions, including pure solvents. Across all cosolvent combinations, including pure solvents, the temperature and PEG 400 mass fractions increased the RCB solubility values. The solubilities of RCB were found to be maximum in pure PEG 400 and minimum in pure water for each temperature under examination. Good agreement was observed between six different computational models and experimentally measured RCB solubility data for all compositions of {PEG 400 + water}, and neat solvents. In both neat solvents and varied mixes of {PEG 400 + water}, all thermodynamic data, including $\Delta_{sol}H°$, $\Delta_{sol}G°$, and $\Delta_{sol}S°$, were demonstrated to be positive, indicating "endothermic and entropy-driven" RCB dissolution. The information gained from this study may help in dosage form design, purification, recrystallization, and pre-formulation evaluation for the RCB.

Acknowledgements
Authors are thankful to the Researchers Supporting Project number (RSPD2025R1040), King Saud University, Riyadh, Saudi Arabia for supporting this work.

Author contributions
Faiyaz Shakeel: Conceptualization, Methodology, Investigation, Software, Resources, Visualization, Funding acquisition, Writing original draft; Ramadan Al-Shdefat: Methodology, Investigation, Formal analysis, Validation, Writing, review, and editing; Mohammad Ali: Formal analysis, Data curation, Validation, Writing, review, and editing; Usama Ahmad: Conceptualization, Methodology, Supervision, Project adinistration, Validation, Writing, review, and editing.

Funding
This work was funded by the Researchers Supporting Project number (RSPD2025R1040), King Saud University, Riyadh, Saudi Arabia.

Data availability
The datasets generated during and/or analysed during the current study are available from the corresponding author on reasonable request.

Declarations

Ethics approval and consent to participate
Not applicable.

Consent for publication
Not applicable.

Competing interests
The authors declare no competing interests.

Clinical trial number
Not applicable.

Received: 13 September 2024 / Accepted: 18 March 2025
Published online: 26 March 2025

References

1. Samant TS, Dhuria S, Lu Y, Laisney M, Yang S, Grandeury A, Mueller-Zsigmondy M, Umehara K, Huth F, Miller M, et al. Ribociclib bioavailability is not affected by gastric pH changes or food intake: in Silico and clinical evaluations. Clin Pharmacol Ther. 2018;104:374–83.
2. U.S. Food and Drug Administration. Ribociclib (Kisqali) | FDA. Available from: https://www.fda.gov/drugs/resources-information-approved-drugs/ribociclib-kisqali. Accessed on 20 May 2024.
3. Shah A, Bloomquist E, Tang S, Fu W, Bi Y, Liu Q, Yu J, Zhao P, Palmby TR, Goldberg KB, et al. FDA approval: ribociclib for the treatment of postmenopausal women with hormone receptor-positive, HER2-negative advanced or metastatic breast cancer. Clin Cancer Res. 2018;24:2999–3004.
4. Yardley DA. Monaleesa clinical program: A review of ribociclib use in different clinical settings. Future Oncol. 2019;15:2673–86.
5. Infante JR, Cassier PA, Gerecitano JF, Witteveen PO, Chugh R, Ribrag V, Chakraborty A, Matano A, Dobson JR, Crystal AS, et al. A phase I study of the cyclin-dependent kinase 4/6 inhibitor ribociclib (LEE011) in patients with advanced solid tumors and lymphomas. Clin Cancer Res. 2016;22:5696–705.
6. Bharate SS. Recent developments in pharmaceutical salts: FDA approvals from 2015 to 2019. Drug Discov Today. 2021;26:384–98.
7. Di L, Fish PV, Mano T. Bridging solubility between drug discovery and development. Drug Discov Today. 2012;17:486–95.
8. Rezaei H, Rahimpour E, Zhao H, Martinez F, Barzegar-Jalali M, Jouyban A. Solubility of Baclofen in some neat and mixed solvents at different temperatures. J Mol Liq. 2022;347:E118352.
9. Barrett JA, Yang W, Skolnik SM, Belliveau LM, Patros KM. Discovery solubility measurement and assessment of small molecules with drug development in Mind. Drug Discov Today. 2022;27:1315–25.
10. Soliman ME, Adewumi AT, Akawa OB, Subair TI, Okunlola FO, Akinsuku AE, Khan S. Simulation models for prediction of bioavailability of medicinal drugs-the interface between experiment and computation. AAPS PharmSciTech. 2022;23:E86.
11. Yadav K, Sachan AK, Kumar S, Dubey A. Techniques for increasing solubility: A review of conventional and new strategies. Asian J Pharm Res Dev. 2022;10:144–53.
12. Jouyban A. Review of the cosolvency models for predicting drug solubility in solvent mixtures: an update. J Pharm Pharm Sci. 2019;22:466–85.
13. Bolla G, Nangia A. Pharmaceutical cocrystals: walking the talk. Chem Commun. 2016;52:8342–60.
14. Bolla G, Sarma B, Nangia AK. Crystal engineering of pharmaceutical cocrystals in the discovery and development of improved drugs. Chem Rev. 2022;122:11514–603.
15. Duggirala NK, Perry ML, Almarsson O, Zaworotko MJ. Pharmaceutical cocrystals: along with the path to improve medicines. Chem Commun. 2016;52:640–55.
16. Paus R, Hart E, Ji Y, Sadowski G. Solubility and caloric properties of Cinnarizine. J Chem Eng Data. 2015;60:2256–61.
17. Ruether F, Sadowski G. Modeling the solubility of pharmaceuticals in pure solvents and solvent mixtures for drug process design. J Pharm Sci. 2009;98:4205–15.
18. Alyamani M, Alshehri S, Alam P, Wani SUD, Ghoneim MM, Shakeel F. Solubility and solution thermodynamics of raloxifene hydrochloride in various (DMSO + water) compositions. Alexand Eng J. 2022;61:9119–28.
19. Al-Shdefat R, Hailat M, Alshogran OY. Solubilization of a novel antitumor drug ribociclib in water and ten different organic solvents at different temperatures. Drug Dev Ind Pharm. 2022;48:12–20.
20. Shakeel F, Haq N, Alsarra IA, Alshehri S, Solubility. Hansen solubility parameters and thermodynamic behavior of emtricitabine in various (polyethylene glycol-400 + water) mixtures: computational modeling and thermodynamics. Molecules. 2020;25:E1559.
21. Rahimpour E, Mohammadian E, Acree WE Jr, Jouyban A. Computational tools for solubility prediction of celecoxib in the binary solvent systems. J Mol Liq. 2020;299:E112129.
22. Moradi M, Rahimpour E, Hemmati S, Martinez F, Barzegar-Jalali M, Jouyban A. Solubility of mesalazine in polyethylene glycol 400 + water mixtures at different temperatures. J Mol Liq. 2020;314:E113546.
23. Alshehri S, Shakeel F, Alam P, Jouyban A, Martinez F. Solubility of 6-phenyl-4,5-dihydropyridazin-3(2H)-one in aqueous mixtures of transcutol and PEG 400 revisited: correlation and Preferential solvation. J Mol Liq. 2021;344:E117728.
24. Alqarni MH, Haq N, Alam P, Abdel-Kader MS, Foudah AI, Shakeel F. Solubility data, Hansen solubility parameters and thermodynamic behavior of pterostilbene in some pure solvents and different (PEG-400 + water) cosolvent compositions. J Mol Liq. 2021;331:E115700.
25. Alghaith AF, Mahdi MA, Haq N, Alshehri S, Shakeel F. Solubility and thermodynamic properties of febuxostat in various (PEG 400 + water) mixtures. Materials. 2022;15:E7318.
26. Shakeel F, Alshehri S, Ghoneim MM, Martinez F, Pena M, Jouyban A, Acree WE. Solubility of Tadalafil in aqueous mixtures of Transcutol® and PEG 400 revisited: correlation, thermodynamics and Preferential solvation. Phys Chem Liq. 2022;60:750–66.
27. Ha ES, Park H, Lee SK, Kang HT, Jeong JS, Kim MS. Equilibrium solubility, solvent effect, and equation correlations of cyclosporine in Twenty mono solvents and four binary mixtures. J Mol Liq. 2024;399:E124389.
28. Higuchi T, Connors KA. Phase-solubility techniques. Adv Anal Chem Instr. 1965;4:117–22.
29. Kamble S, Munipalli V, Talapadatur H, Singh RM, Warde S, Nayak S, Vaidhun B. Development and validation of novel HPLC method for analytical evaluation of ribociclib. Int J Pharm Pharm Res. 2021;22:510–25.
30. Shakeel F, Alshehri S, Solubilization. Hansen solubility parameters, solution thermodynamics and solvation behavior of flufenamic acid in (Carbitol + water) mixtures. Processes. 2020;8:E1204.
31. Shakeel F, Haq N, Alanazi FK, Alanazi SA, Alsarra IA. Solubility of sinapic acid in various (Carbitol + water) systems: computational modeling and solution thermodynamics. J Therm Anal Calorim. 2020;142:1437–46.
32. Alshehri S, Shakeel F. Solubility determination, various solubility parameters and solution thermodynamics of Sunitinib malate in some cosolvents, water and various (Transcutol + water) mixtures. J Mol Liq. 2020;307:E112970.
33. Zhu QN, Wang Q, Hu YB, Abliz X. Practical determination of the solubility parameters of 1-alkyl-3-methylimidazolium bromide ([CnC1im]Br, n = 5, 6, 7, 8) ionic liquids by inverse gas chromatography and the Hansen solubility parameter. Molecules. 2019;24:E1346.

34. Alanazi A, Alshehri S, Altamimi M, Shakeel F. Solubility determination and three dimensional Hansen solubility parameters of gefitinib in different organic solvents: experimental and computational approaches. J Mol Liq. 2020;299:E112211.
35. Kalam MA, Alshamsan A, Alkholief M, Alsarra IA, Ali R, Haq N, Anwer MK, Shakeel F. Solubility measurement and various solubility parameters of glipizide in different neat solvents. ACS Omega. 2020;5:1708–16.
36. Wan Y, He H, Huang Z, Zhang P, Sha J, Li T, Ren B. Solubility, thermodynamic modeling and Hansen solubility parameter of 5-norbornene-2,3-dicarboximide in three binary solvents (methanol, ethanol, Ethyl acetate + DMF) from 278.15 K to 323.15 K. J Mol Liq. 2020;300:E112097.
37. Ruidiaz MA, Delgado DR, Martínez F, Marcus Y. Solubility and Preferential solvation of indomethacin in 1,4-dioxane + water solvent mixtures. Fluid Phase Equilib. 2010;299:259–65.
38. Hildebrand JH, Prausnitz JM, Scott RL. Regular and related solutions. New York: Van Nostrand Reinhold; 1970.
39. Manrique YJ, Pacheco DP, Martínez F. Thermodynamics of mixing and solvation of ibuprofen and Naproxen in propylene glycol + water cosolvent mixtures. J Sol Chem. 2008;37:165–81.
40. Apelblat A, Manzurola E. Solubilities of o-acetylsalicylic, 4-aminosalicylic, 3,5-dinitrosalicylic and p-toluic acid and magnesium-DL-aspartate in water from T = (278–348) K. J Chem Thermodyn. 1999;31:85–91.
41. Manzurola E, Apelblat A. Solubilities of L-glutamic acid, 3-nitrobenzoic acid, acetylsalicylic, p-toluic acid, calcium-L-lactate, calcium gluconate, magnesium-DL-aspartate, and magnesium-L-lactate in water. J Chem Thermodyn. 2002;34:1127–36.
42. Ksiazczak A, Moorthi K, Nagata I. Solid-solid transition and solubility of even n-alkanes. Fluid Phase Equilib. 1994;95:15–29.
43. Tong Y, Wang Z, Yang E, Pan B, Jiang J, Dang P, Wei H. Determination and correlation of solubility and solution thermodynamics of Ethenzamide in different pure solvents. Fluid Phase Equilib. 2016;427:549–56.
44. Yalkowsky SH, Roseman TJ. Solubilization of drugs by cosolvents. In: Yalkowsky SH, editor. Techniques of solubilization of drugs. New York: Marcel Dekker Inc; 1981. pp. 91–134.
45. Jouyban A, Acree WE Jr. Mathematical derivation of the Jouyban-Acree model to represent solute solubility data in mixed solvents at various temperatures. J Mol Liq. 2018;256:541–7.
46. Shakeel F, Bhat MA, Haq N, Fathi-Azarbayjani A, Jouyban A. Solubility and thermodynamic parameters of a novel anti-cancer drug (DHP-5) in polyethylene glycol 400 + water mixtures. J Mol Liq. 2017;229:241–5.
47. Krug RR, Hunter WG, Grieger RS. Enthalpy-entropy compensation. 2. Separation of the chemical from the statistic effect. J Phys Chem. 1976;80:2341–51.
48. Holguín AR, Rodríguez GA, Cristancho DM, Delgado DR, Martínez F. Solution thermodynamics of indomethacin in propylene glycol + water mixtures. Fluid Phase Equilib. 2012;314:134–9.

Publisher's note